Midday magnetopause shifts earthward of geosynchronous orbit during geomagnetic superstorms with Dst ≤ −300 nT

H. Li,[1,2] C. Wang,[1] and J. R. Kan[1,3]

Received 28 June 2009; revised 2 April 2010; accepted 21 April 2010; published 28 August 2010.

[1] Geomagnetic storm intensity, as measured by the Dst (SYMH) index, shows no limit as the solar wind dawn-to-dusk electric field increases. We show that the magnetopause around noon erodes earthward with increasing storm intensity. The panoramic geosynchronous B_Z signatures for the magnetic storm groups with different intensity are differ significantly from each other. For superstorms with SYMH ≤ −300 nT, the magnetopause around noon erodes to inside the geosynchronous orbit, which causes the B_Z reversal near local noon. The necessary conditions for superstorms with SYMH ≤ −300 nT to occur include the following: (1) interplanetary magnetic field (IMF) B_Z < −27 nT lasts for at least ~1 h; (2) solar wind dynamic pressure, P_d > ~ 12 nPa; (3) the projected interplanetary electric field, E_{K-L} > ~30 mV/m.

Citation: Li, H., C. Wang, and J. R. Kan (2010), Midday magnetopause shifts earthward of geosynchronous orbit during geomagnetic superstorms with Dst ≤ −300 nT, *J. Geophys. Res.*, *115*, A08230, doi:10.1029/2009JA014612.

1. Introduction

[2] As a major type of electromagnetic disturbance in the magnetosphere, geomagnetic storms are of fundamental importance in understanding the space weather and its terrestrial effects. Solar wind can be considered an infinite energy source to power electromagnetic disturbances in the solar wind-magnetosphere-ionosphere (SW-M-I) coupling system. The southward interplanetary magnetic field (IMF) reconnects with the Earth's dipole magnetic field [*Dungey*, 1961], leading to the energy enters into the magnetosphere from the solar wind. The energy from the solar wind would accumulate in the magnetosphere when the rate of energy input is higher than the rate of its quasistationary dissipation and would release when its amount exceeds some certain level, which results in the generation of magnetospheric disturbances, such as geomagnetic storms [*Yermolaev et al.*, 2005]. The rate of energy input depends on the strength and duration of the southward IMF B_Z, together with the solar wind bulk speed [*Meloni et al.*, 2005].

[3] The interplanetary causes of magnetic storms have been investigated for decades [e.g., see *Tsurutani and Gonzalez*, 1997, for a review]. Recently, *Srivastava and Venkatakrishnan* [2004] suggested that the intensity of geomagnetic storms depended strongly on IMF B_Z and $|VB_Z|$, followed by the solar wind dynamic pressure (P_d). The correlation coefficients of B_Z–Dst, $|VBz|$–Dst, and P_d–Dst were 0.70, 0.66, and 0.64, respectively. *Echer et al.* [2008] also showed good linear correlations of the peak Dst with peak values of southward IMF and the dawn to dusk electric field E_Y during the storm main phase.

[4] With the emerging applications of space weather to modern society, very intense magnetic storms (or superstorms) have been paid much attention. Fast ICME magnetic fields, interplanetary shock effects, and double or triple-step storms are suggested to be the major causes of the extreme intense magnetic storms [*Tsurutani et al.*, 1999; *Gonzalez et al.*, 2001, 2002]. *Lopez et al.* [2009] showed that there was no upper limit of the ring current injection rate.

[5] *Gonzalez et al.* [1994] made a summary of the threshold values of the magnitude and duration of southward IMF for magnetic storms with Dst ≥ −200 nT. However, the classification of superstorms is not well defined in the literature. In this study, we will try to identify the interplanetary conditions for superstorms and their signatures in the geosynchronous magnetic field B_Z observed by Geostationary Operational Environmental Satellite (GOES) spacecraft. A new result using the 360° panoramic synthesis technique that the dayside magnetopause moves earthward of the synchronous orbit is found for superstorms with Dst ≤ −300 nT. Therefore, we propose to define the magnetic storms with Dst ≤ −300 nT to be superstorms. The usual conditions on the solar wind dynamic pressure, and the magnitude and duration of southward IMF will be specifically identified.

2. Conditions for Superstorms

[6] *Gonzalez et al.* [1994] suggested that the primary cause of magnetic storms was associated with interplanetary structures with intense, long-duration IMF B_S. The earthward solar wind velocity played another important role in creating geomagnetic storms [*Snyder et al.*, 1963; *Fairfield and Cahill*, 1966]. In addition, solar wind ram pressure made a great contribution to ring current energization,

[1]State Key Laboratory of Space Weather, Center for Space Science and Applied Research, Chinese Academy of Sciences, Beijing, China.
[2]Graduate School of Chinese Academy of Sciences, Beijing, China.
[3]Geophysical Institute, University of Alaska, Fairbanks, Alaska, USA.

0148-0227/10/2009JA014612

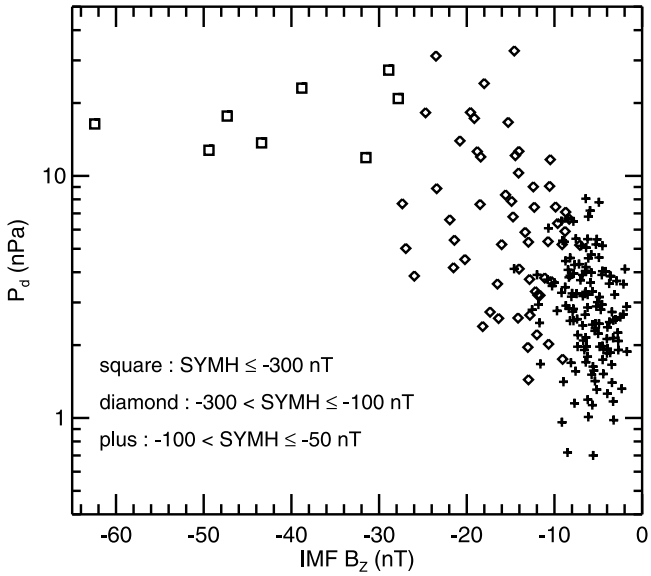

Figure 1. Scatter plots of the solar wind dynamic pressure versus IMF B_Z for three magnetic storm intensity groups. Small to moderate storms with $-100 < \text{SYMH} \leq -50$ nT (crosses); the intense to big storms with $-300 < \text{SYMH} \leq -100$ nT (diamonds); the superstorms with SYMH ≤ -300 nT (squares).

although perhaps less so in substorm progresses [*Gonzalez et al.*, 1989].

[7] We study the 204 magnetic storms (SYMH ≤ -50 nT) during 1998–2005 and obtain the corresponding solar wind dynamic pressure and IMF B_Z at the L1 point observed by ACE spacecraft as the conditions for that storm, when the SYMH index of a storm reaches the minimum. The SYMH of 1 min time resolution is essentially identical to the hourly Dst index. It is worthy of special mention that the SWEPAM instrument on board the ACE spacecraft measures the solar wind speed and ion density every 64s in its "track" mode and takes one measurement every 33 min in a "search" mode. During some superstorms, the "track" model failed to work, but the 33 min resolution "search" mode data are usable [*Hairston et al.*, 2005]. Moreover, we also use the 1 min resolution data from Omni-1 and 1 h resolution data from Omni-2 to supplement the missing data of ACE spacecraft during some superstorms. All the plasma and magnetic field data have been time shifted appropriately. The amount of time shifting here is based on the transit time of the solar wind from the L1 point to the magnetopause using the corresponding solar wind speed and then adding an extra 15 min to account for the response time of magnetosphere [*Ridley et al.*, 1998].

[8] Figure 1 shows the scatter plots of the solar wind dynamic pressure (P_d) versus IMF B_Z for three groups of magnetic storms. Small to moderate storms with $-100 < \text{SYMH} \leq -50$ nT are denoted by the pluses; intense to big storms with $-300 < \text{SYMH} \leq -100$ nT are denoted by the diamonds; superstorms with SYMH ≤ -300 nT are denoted by the squares. Note that regions for the three magnetic storm groups are separated from each other clearly on the plot. The value of B_Z seems to be more reliable in distinguishing these three groups; however, the P_d value could not be left out. A general trend is that the IMF B_Z needs to be more southward and solar wind dynamic pressure needs to be larger as the storm intensity increases. Figure 1 shows clearly that superstorms depend more on condition (1) IMF $B_Z < -27$ nT than condition (2) solar wind dynamic pressure $P_d > \sim 12$ nPa. By studying superstorms further case by case, we found that the duration of IMF $B_Z < -27$ nT must last for at least ~1 h.

[9] Next we will try to find the relationship between the storm intensity and the interplanetary electric field (IEF). Instead of using the dawn to dusk electric field, we consider the projected interplanetary electric field $V_X B_{YZ} \sin^2(\theta/2)$ (or E_{K-L}), where θ is the IMF clock angle, V_X is the x component of solar wind speed, and B_{YZ} is the IMF projection on the YZ plane, suggested by *Kan and Lee* [1979], which has been illustrated to be effective by *Burke et al.* [1999] in their discussion of the implicit relationship between geoeffective scale sizes in the interplanetary medium and electric potentials imposed on the ionosphere across the polar cap. Figure 2 plots the storm intensity, measured by the midlatitude symmetric geomagnetic index SYMH against the projected interplanetary electric field E_{K-L}. Within the observed range of E_{K-L}, the storm intensity clearly increases linearly with increasing E_{K-L}. The empirical formula for the relationship between the magnetic storm intensity and the projected interplanetary electric field is shown as follows:

$$-\text{SYMH} = 9.68 \times E_{K-L} + 20.07.$$

When $E_{K-L} = 0$, the SYMH will not equal 0 due to the contribution of "viscous interaction" [*Axford and Hines*, 1961]. When E_{K-L} exceeds ~30 mV/m, superstorm would occur. *Wang et al.* [2003] showed the necessary conditions on $-VB_Z$ and its duration Δt. As Δt increases, the condition on $-VB_Z$ for superstorms (SYMH = −300 nT) has a wide range. Actually, a stronger $-VB_Z$ can produce a more intense storm, whereas a longer Δt cannot.

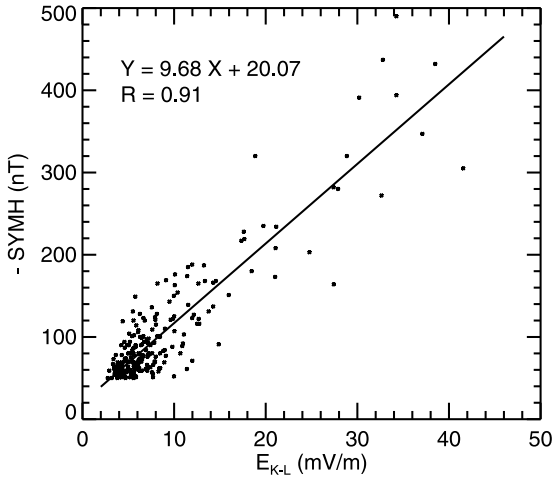

Figure 2. The dependence of storm intensity measured by the SYMH index on the projected interplanetary electric field (E_{K-L}) for the geomagnetic storms during 1998–2005.

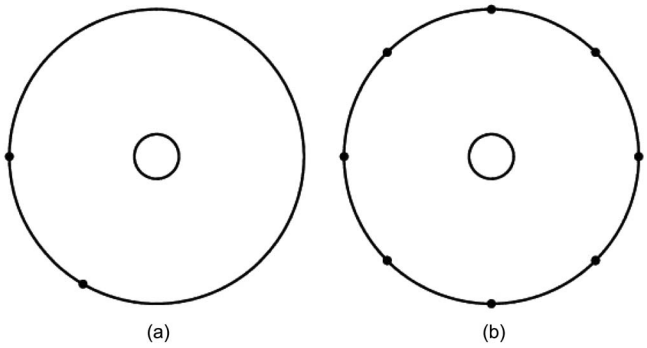

Figure 3. (a) Point observation of geosynchronous magnetic fields during a storm; (b) Panoramic observation of geosynchronous magnetic field during the similar intensity of storms.

[10] In summary, we identify specific physical conditions for the occurrence of superstorms with SYMH ≤ -300 nT as follows: (1) IMF $B_Z < -27$ nT lasts for at least ~1 h; (2) solar wind dynamic pressure, $P_d >$ ~12 nPa; and (3) the projected interplanetary electric field, $E_{K-L} >$ ~30 mV/m.

3. Panoramic Geosynchronous B_Z Signature

[11] Geomagnetic storm is a global phenomenon in the inner magnetosphere produced by the SW-M-I coupling. In the present paper, we use a statistical method to obtain 360° panoramic views of geosynchronous B_Z signature during storms of different intensities.

[12] We studied 196 small to big storms ($-300 <$ SYMH ≤ -50 nT) from 1998 to 2005 and 15 superstorms during 1989–2005. When SYMH reaches its minimum, we take the corresponding 10 min averaged B_Z value from GOES spacecraft for that storm. For example, if there are two GOES spacecrafts in the synchronous orbit, two data points with different local time are obtained for a given storm, as illustrated in Figure 3a. We divide all the storms into the same three groups as in section 2. There are enough cases of geomagnetic storms for each group to cover all local times. The geostationary B_Z versus all local times is defined as the panoramic signature of geosynchronous B_Z during storms in each of the three groups, as shown in Figure 3b. All the geosynchronous magnetic field data are obtained from GOES-6 (1989–1992), GOES-7 (1989–1992), GOES-8 (January 1997–April 2003), GOES-10 (Match 1999– December 2005), and GOES-12 (April 2003–December 2005).

[13] The panoramic geosynchronous B_Z signatures for the three magnetic storm groups are differ significantly from each other. Figure 4a shows the panoramic geosynchronous B_Z signature for small to moderate storms. It is clear that B_Z varies smoothly with local time, peaking prenoon (~11:00 LT) and reducing to the nightside. The distribution of B_Z is similar to a Gaussian distribution, and the solid curve is obtained by the Gaussian curve fitting, and the parameter R^2 represents the goodness of Gaussian fitting. The closer the R^2 approach to 1, the better the Gaussian fit is. For intense to big storms, shown in Figure 4b, the B_Z signature is slightly different from the previous one. The bell-shaped distribution becomes flatter; meanwhile, the overall appearance of B_Z is less than that shown in Figure 4a. For example, the mean maximum value of B_Z near local noon is ~85 nT, and the mean value of B_Z near local night is ~30 nT. By contrast, the corresponding values for small to moderate storms are ~110 and ~40 nT, respectively. This phenomenon is understandable. Let examine cases of nightside first; as the storm intensity increases, the cross-tail current becomes stronger and closer to Earth, resulting in a smaller geosynchronous B_Z on the nightside. As for the dayside, the increased Region-1 current makes the geosynchronous B_Z smaller [*Siscoe et al.*, 2002]. The geosynchronous B_Z signature for superstorms is shown in Figure 4c. Compared to the previous two cases, the difference is significant. The Gaussian-like distribution even reverses, with a southward geosynchronous B_Z during 9:00–15:00 LT. During superstorms, the dayside magnetopause shifts earthward of the geosynchronous orbit. The southward magnetic field in the magnetosheath and the southward field of the Chapman-Ferraro current, cause the B_Z reversal near local noon. Therefore, we propose to define the magnetic storms with Dst ≤ -300 nT to be superstorms.

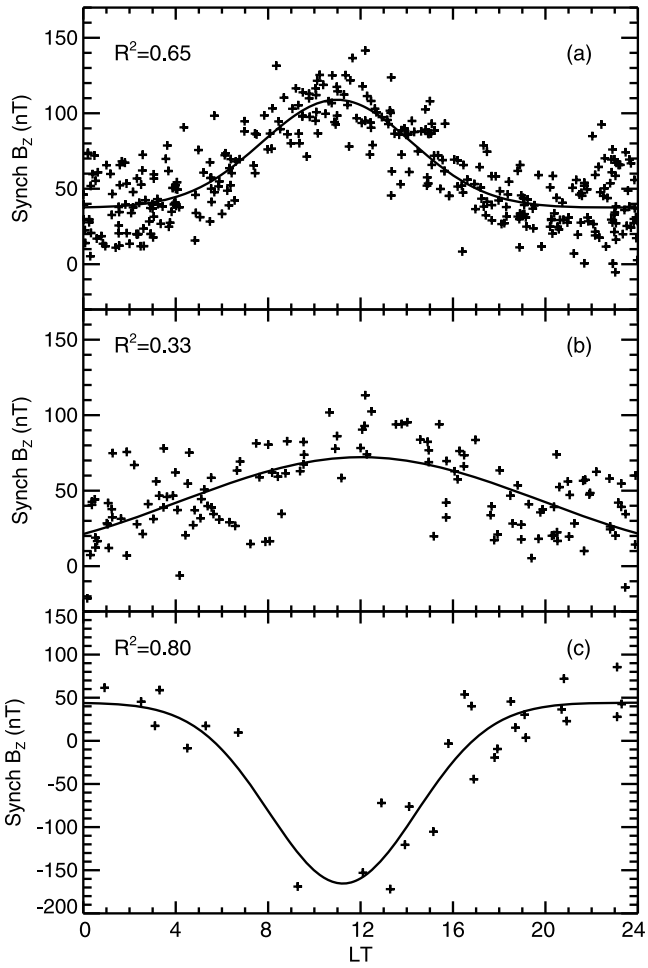

Figure 4. Geosynchronous B_Z versus local time (LT) for three groups of magnetic storms: (a) small to moderate storms; (b) intense to big storms; and (c) superstorms. The solid curve is the Gaussian curve fitting.

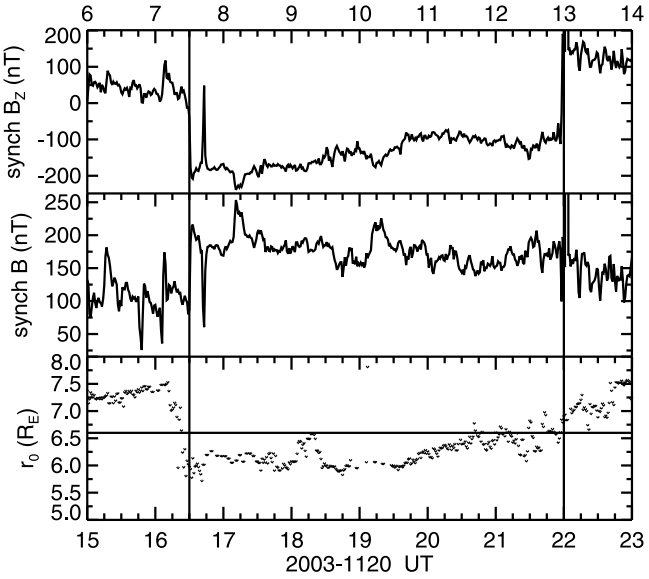

Figure 5. An example of the dayside magnetopause shifting earthward of the geosynchronous orbit during the 20 November 2003 superstorm with SYMH = −490 nT, measured by GOES-10. (top) The geosynchronous magnetic filed Z component, B_Z; (middle) the magnitude of the geosynchronous magnetic field, B; (bottom) the subsolar standoff distance of the magnetopause derived from the model of *Shue et al.* [1998]. The top axis labels the corresponding local time of GOES-10.

[14] Figure 5 shows an example of the dayside magnetopause shifting earthward of the geosynchronous orbit during the 20 November 2003 superstorm with SYMH = −490 nT, measured by GOES-10. Figures 5 (top), 5 (middle), and 5 (bottom) show, respectively, the geosynchronous magnetic field Z component, B_Z; the magnitude of the geosynchronous magnetic field, B; and the subsolar standoff distance of the magnetopause derived from the model of *Shue et al.* [1998]. The top axis labels the corresponding local time of GOES-10. Vertical lines indicate magnetosheath entrances and exits, respectively. At about 16:30 UT (7:30 LT), B_Z suddenly changed direction from northward to southward and then returned to northward at about 22:00 UT (13:00 LT). At the corresponding time, the magnitude of the geosynchronous magnetic field shows similar sudden changes. The significant deviation of geosynchronous magnetic field from geomagnetic field conclusively demonstrates that the GOES-10 satellite was indeed in the magnetosheath during 16:30 UT–22:00 UT. As further proof, the subsolar location of the magnetopause, derived from the model of *Shue et al.* [1998], was within 6.6 R_E during that time period. Similarly, we find that the dayside magnetopause shifted within the geostationary orbit for other superstorms as well.

[15] In addition to the strong deviation of the geosynchronous magnetic field measured by GOES, the significant change of other parameters, such as the integral electron flux (>0.6 MeV), measured by GOES could further confirm that the dayside magnetopause shifts earthward of geosynchronous orbit during superstorms. As an example, Figure 6 shows the profiles of integral electron flux (>0.6 MeV) and geosynchronous B_Z observed during a superstorm with SYMH = −320 nT on 6 April 2000. The integral electron flux observed by GOES-10 and by SOHO at the L1 point are plotted with a solid line and dashed line, respectively, in Figure 6 (top). The geosynchronous magnetic field B_Z is plotted in the bottom panel. Vertical dot lines mark the magnetosheath entrance and exit, as indicated by the sudden change of geosynchronous B_Z. At about 18:00 UT (9:00 LT), the integral electron flux observed by GOES-10 suddenly changed from 10^5 to 10^1, about the same order of that observed by SOHO at the L1 point, which implies that the GOES-10 was located outside the magnetopause. At about 00:25 UT (15:25 LT) on 7 April, the value returned to 10^3 again, back to inside the magnetopause.

[16] Both the solar wind dynamic pressure (P_d) and IMF B_Z can contribute to the earthward motion of the dayside magnetopause. If the P_d reached a certain high level, the magnetopause can also move to locations within 6.6 R_E, even during northward IMF B_Z. In addition to superstorms, there are other 11 geomagnetic storms during 1998–2005, ranging from −116 to −280 nT, which could make the dayside magnetopause shift within the synchronous orbit as well. For these storms, the IMF B_Z ranged from −10 to −23 nT, and the main cause was the extremely large solar wind dynamic pressure P_d. As for the relative importance of IMF B_Z parameter versus the solar wind dynamic pressure P_d parameter in defining the magnetopause shifts, *Yang et al.* [2003] proposed that the response of magnetopause to IMF B_Z and solar wind dynamic pressure P_d should be nonlinear, especially when the magnetopause is close to Earth. The earthward motion of magnetopause due to south-

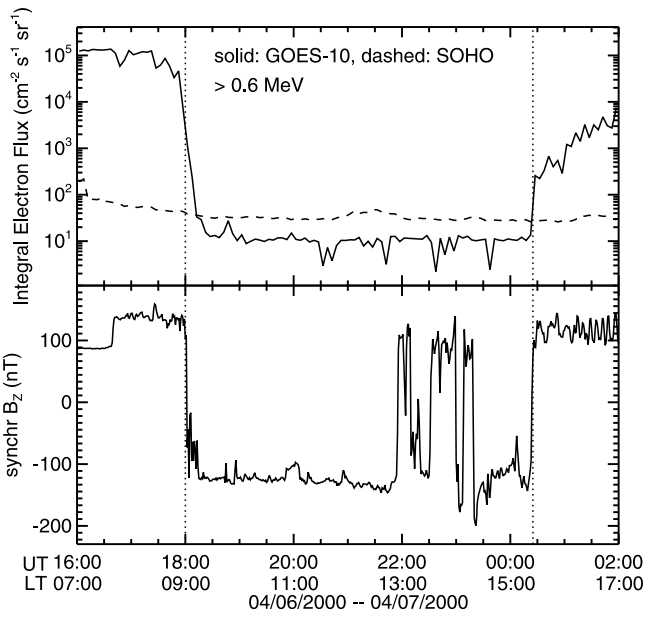

Figure 6. One example of the dayside magnetopause shifting earthward of the geosynchronous orbit during a superstorm with SYMH = −320 nT on 06 April 2000. The profiles of (top) integral electron flux (>0.6 MeV) and (bottom) geosynchronous magnetic filed Z component, B_Z.

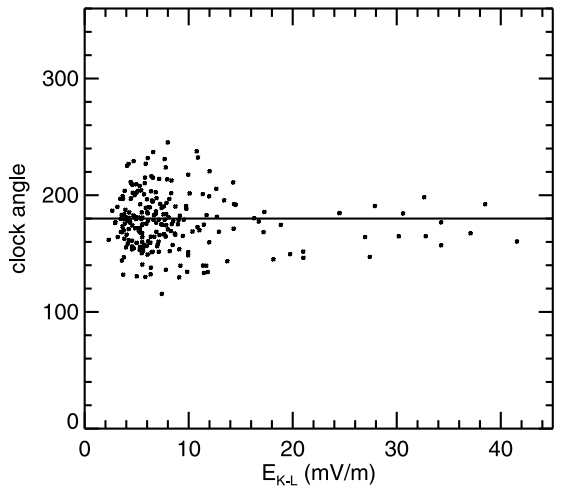

Figure 7. The relation between the maximum of the projected interplanetary electric field (E_{K-L}) for magnetic storms and the corresponding clock angle.

ward IMF B_Z should be saturated, and the threshold of B_Z for saturation occurring should be related with P_d.

4. Discussion and Summary

[17] Geomagnetic storms involve energy storage in the ring current, which is transport to the inner magnetosphere by sunward convection in the plasma sheet, driven by the solar wind through dayside and nightside magnetic reconnections. A larger southward IMF B_Z and solar wind dynamic pressure can result in more intense magnetic reconnection. A longer duration of southward IMF B_Z can transfer more energy to the magnetosphere by magnetic reconnection. Pure southward IMF exists only in the numerical simulation. The effect of IMF clock angle should not be overlooked. Figure 7 shows the relation between the maximum of the projected interplanetary electric field for magnetic storms and the corresponding clock angle. The range of clock angle reduces as the storm intensity increases. For small to moderate storms ($E_{K-L} < \sim 10$ mV/m), the clock angle scatters over a wide range from 120° to 240°. The range for superstorms ($E_{K-L} > \sim 30$ mV/m) is reduced to 160° to 200°.

[18] We identify specific physical conditions for the occurrence of superstorms. These conditions are summarized as follows: (1) IMF $B_Z < -27$ nT lasts for at least ~1 h; (2) solar wind dynamic pressure, $P_d > \sim 12$ nPa; and (3) the projected interplanetary electric field, $E_{K-L} > \sim 30$ mV/m. The 360° panoramic views of geosynchronous B_Z signature for storms of different intensities differ significantly from each other. For small to moderate ($-100 < \mathrm{SYMH} \leq -50$ nT), the distribution of geosynchronous magnetic B_Z versus the local time is very similar to a Gaussian distribution, with a peak prenoon. As the magnetic storm intensity increases, the Gaussian-like distribution becomes flatter for intense to big storms ($-300 < \mathrm{SYMH} \leq -100$ nT) and even reverses during superstorms with Dst ≤ -300 nT, which implies that the midday magnetopause is located earthward of the geosynchronous orbit. Note that the midday magnetopause can also shift inside of the geosynchronous orbit when the solar wind dynamic pressure is extreme large, without superstorms, if conditions (1), (2), and (3) are not satisfied simultaneously.

[19] **Acknowledgments.** We acknowledge the use of data from ACE, SOHO, and GOES experiments teams. We also thank the Kyoto World Data Center for providing the ASY/SYM indices. This work was supported by grants NNSFC 40621003 and 40831060 and in part by the Specialized Research Fund for State Key Laboratories of China.

[20] Zuyin Pu thanks the reviewers for their assistance in evaluating this paper.

References

Axford, W. I., and C. O. Hines (1961), A unifying theory of high-latitude geophysical phenomena and geomagnetic storms, *Can. J. Phys.*, *39*, 1433.

Burke, W. J., D. R. Weimer, and N. C. Maynard (1999), Geoeffective interplanetary scale sizes derived from regression analysis of polar cap potentials, *J. Geophys. Res.*, *104*(A5), 9989–9994.

Dungey, J. W. (1961), Interplanetary magnetic field and the auroral zones, *Phys. Rev. Lett.*, *6*, 47–48.

Echer, E., W. D. Gonzalez, B. T. Tsurutani, and A. L. C. Gonzalez (2008), Interplanetary Conditions Causing Intense Geomagnetic Storms (Dst $\leq$ −100 nT) during solar cycle 23(1996–2006), *J. Geophys. Res.*, *113*, A05221, doi:10.1029/2007JA012744.

Fairfield, D. H., and L. J. Cahill (1966), Transition region magnetic field and polar magnetic disturbances, *J. Geophys. Res.*, *71*(1), 155–169.

Gonzalez, W. D., B. T. Tsurutani, A. L. Clua de Gonzalez, F. Tang, E. J. Smith, and S. I. Akasofu (1989), Solar wind-magnetosphere coupling during intense geomagnetic storms (1978–1979), *J. Geophys. Res.*, *94*(A7), 8835–8851.

Gonzalez, W. D., J. A. Joselyn, Y. Kamide, H. W. Kroehl, G. Rostoker, B. T. Tsurutani, and V. M. Vasyliunas (1994), What is a geomagnetic storm?, *J. Geophys. Res.*, *99*(A4), 5771–5792.

Gonzalez, W. D., A. L. Clua de Gonzalez, J. H. A. Sobral, A. Dal Lago, and L. E. Vieira (2001), Solar and interplanetary causes of very intense geomagnetic storms, *J. Atmos. Sol. Terr. Phys.*, *63*, 403–412.

Gonzalez, W. D., B. T. Tsurutani, R. P. Lepping, and R. Schwenn (2002), Interplanetary phenomena associated with very intense geomagnetic storms, *J. Atmos. Sol. Terr. Phys.*, *64*, 173–181.

Hairston, M. R., K. A. Drake, and R. Skoug (2005), Saturation of the ionospheric polar cap potential during the OctoberCNovember 2003 superstorms, *J. Geophys. Res.*, *110*, A09S26, doi:10.1029/2004JA010864.

Kan, J. R., and L. C. Lee (1979), Energy coupling function and solar wind-magnetosphere dynamo, *Geophys. Res. Lett.*, *6*(7), 577–580.

Lopez, R. E., J. G. Lyon, E. Mitchell, R. Bruntz, V. G. Merkin, S. Brogl, F. Toffoletto, and M. Wiltberger (2009), Why doesn't the ring current injection rate saturate?, *J. Geophys. Res.*, *114*, A02204, doi:10.1029/2008JA013141.

Meloni, A., P. De Mechelis, and R. Tozzi (2005), Geomagnetic storms, dependence on solar and interplanetary phenomena: A review, *Mem. Soc. Astron. Ital.*, *76*, 882–887.

Ridley, A. J., G. Lu, C. R. Clauer, and V. O. Papitashvili (1998), A statistical study of the ionospheric convection response to changing interplanetary magnetic field conditions using the assimilative mapping of ionospheric electrodynamics technique, *J. Geophys. Res.*, *103*(A3), 4023–4039.

Shue, J.-H., et al. (1998), Magnetopause location under extreme solar wind conditions, *J. Geophys. Res.*, *103*(A8), 17,691–17,700.

Siscoe, G. L., N. U. Crooker, and K. D. Siebert (2002), Transpolar potential saturation: Roles of region 1 current system and solar wind ram pressure, *J. Geophys. Res.*, *107*(A10), 1321, doi:10.1029/2001JA009176.

Snyder, C. W., M. Neugebauer, and V. R. Rao (1963), The solar wind velocity and its correlation with solar and geomagnetic activity, *J. Geophys. Res.*, *68*, 6361–6370.

Srivastava, N., and P. Venkatakrishnan (2004), Solar and interplanetary sources of major geomagnetic storms during 1996–2002, *J. Geophys. Res.*, *109*, A10103, doi:10.1029/2003JA010175.

Tsurutani, B. T., and W. D. Gonzalez (1997), Interplaneatry causes of magnteic storms: A review, in *Magnetic Storms*, *Geophys. Monogr. Ser.*, vol. 98, edited by B. T. Tsurutani et al., pp. 77, AGU, Washington, D. C.

Tsurutani, B. T., Y. Kamide, J. K. Arballo, W. D. Gonzalez, and R. P. Lepping (1999), Interplanetary causes of great and superintense magnetic storms, *Phys. Chem. Earth C*, *24*, 101–105.

Wang, Y. M., C. L. Shen, S. Wang, and P. Z. Ye (2003), An empirical formula relating the geomagnetic storm's intensity to the interplanetary parameters: $-\overline{VB_Z}$ and Δt, *Geophys. Res. Lett.*, *30*(20), 2039, doi:10.1029/2003GL017901.

Yang, Y.-H., J. K. Chao, A. V. Dmitriev, C.-H. Lin, and D. M. Ober (2003), Saturation of IMF B_Z influence on the position of dayside magnetopause, *J. Geophys. Res.*, *108*(A3), 1104, doi:10.1029/2002JA009621.

Yermolaev, Y. I., M. Y. Yermolaev, G. N. Zastenker, L. M. Zelenyi, A. A. Petrukovich, and J.-A. Sauvaud (2005), Statistical studies of geomagnetic storm dependencies on solar and interplanetary events: A review, *Planet. Space Sci.*, *53*, 189–196.

J. R. Kan, Geophysical Institute, University of Alaska Fairbanks, 903 Koyukuk Dr., Fairbanks, AK 99775-7320, USA. (joe.kan@gi.alaska.edu)

H. Li and C. Wang, State Key Laboratory of Space Weather, Center for Space Science and Applied Research, Chinese Academy of Sciences, PO Box 8701, Beijing 100190, China. (hli@spaceweather.ac.cn; cw@spaceweather.ac.cn)